Available online at www.sciencedirect.com
SCIENCE DIRECT®
Journal of Solid State Chemistry 177 (2004) 642–647
JOURNAL OF SOLID STATE CHEMISTRY
http://elsevier.com/locate/jssc

Inorganic–organic hybrid compounds: hydrothermal synthesis and characterization of a new three-dimensional metal tetraphosphonate $Mn[(HO_3PCH_2)N(H)(CH_2)_4(H)N(CH_2PO_3H)_2]$

Norbert Stock,* Max Rauscher, and Thomas Bein

Department Chemie, Ludwig-Maximilians-Universität München, Butenandtstr. 5-13 (Haus E), München 81377, Germany

Received 5 June 2003; received in revised form 30 July 2003; accepted 1 August 2003

Abstract

The new manganese tetraphosphonate, $Mn[(HO_3PCH_2)_2N(H)(CH_2)_4(H)N(CH_2PO_3)_2]$ (**1**) was hydrothermally synthesized from $MnCl_2$ and *N*,*N*,*N*′,*N*′-tetrametylphosphono-1,4-diaminobutane, $(H_2O_3PCH_2)_2N–(CH_2)_4–N(CH_2PO_3H_2)_2$. The structure was determined from single-crystal X-ray diffraction data ($Mn[(HO_3PCH_2)_2N(H)(CH_2)_4(H)N(CH_2PO_3)_2]$, monoclinic, $P2_1/a$, with $a = 9.6663(1)$, $b = 9.2249(2)$, $c = 10.5452(1)$ pm, $\beta = 105.676(1)°$, $V = 905.35(3) \times 10^6$ pm, $Z = 2$, $R_1 = 0.051$, w$R_2 = 0.109$ (all data). The structure contains the zwitter ions $[(HO_3PCH_2)_2N(H)–(CH_2)_4–(H)N(CH_2PO_3)_2]^{2-}$ and is built from alternating corner-linked $[MnO_6]$ and $[PO_3C]$ polyhedra forming a two-dimensional net of eight-rings. These layers are connected to a pillared structure by the diaminobutane groups. Magnetic susceptibility data confirms the presence of Mn^{2+} ions. Thermogravimetric measurements show a stability of **1** up to ~290°C. Between 290°C and 345°C a one-step loss of ~7.0% is observed, and above 345°C the continuous decomposition of the organic part of the structures takes place.

Keywords: Manganese; Phosphonate; Hydrothermal synthesis; Crystal structure; Magnetic properties

1. Introduction

Hybrid materials with organic and inorganic moieties are an attractive field of research due to their composite properties and the possibility of tuning their chemistry [1]. The potential of these inorganic–organic hybrid materials lies in their use as sorbents, ion exchangers, catalysts or charge storage materials. The use of bifunctional anionic units in this field [2], e.g., diphosphonates ($[O_3P–R–PO_3]^{4-}$) [3], aminophosphonates ($[O_3P–R–NH_2]^{2-}$) [4], and phosphonocarboxylates ($[O_3P–R–COO]^{3-}$) [5], has lead to many new three-dimensional compounds of di-, tri- and tetra-valent metals.

Whereas a vast number of inorganic–organic hybrid materials with mono- and diphosphonates have been described, little is known about tri- and other polyphosphonate compounds. In recent publications the use of nitrilotris(methylene)triphosphonic acid has been described. Thus, three lead nitrilotris(methylene)-triphosphonates $Pb[(H_2O_3PCH_2)N(CH_2PO_3H)_2]$, $Pb_2[(O_3PCH_2)N(CH_2PO_3H)_2]\cdot H_2O$, $Pb_2[(O_3PCH_2)N(CH_2PO_3H)_2]$ [6], a number of isostructural, pure and mixed metal phosphonates $M[(HO_3PCH_2)_3NH)]\cdot 3H_2O$ [7] (M = Co, Mn, Ni, Zn, Cu, Cd), $Al[(HO_3PCH_2)_3N]\cdot H_2O$ [8] and $Na_2[(HO_3PCH_2)_3NH]\cdot 1.5H_2O$ [9] have been obtained.

We are interested in the use of multi-functionalized phosphonic and phosphonocarboxylic acids and their use in the synthesis of inorganic–organic hybrid compounds. Thus, the use of the diphosphonic acid $H_2O_3PCH_2C_6H_4CH_2PO_3H_2$ has led to the following compounds: $Pb_2[O_3PCH_2C_6H_4CH_2PO_3]$ [10], $Sn_2[O_3PCH_2C_6H_4CH_2PO_3]$ [11], and the isostructural transition metal diphosphonates $M_2[O_3PCH_2C_6H_4CH_2PO_3]\cdot 2H_2O$ (M = Mn, Ni, Cd) [12]. We have recently started a systematic investigation on the applicability of aminomethylenephosphonic acids in the synthesis of metal phosphonates since these phosphonic acids can be readily prepared by a Mannich-type reaction using

*Corresponding author. Fax: +49-89-2180-7622.
E-mail address: norbert.stock@cup.uni-muenchen.de, nstch@cup.uni-muenchen.de (N. Stock).

0022-4596/$ - see front matter © 2003 Elsevier Inc. All rights reserved.
doi:10.1016/j.jssc.2003.08.005

primary and secondary amines, formaldehyde and phosphoric acid as starting materials [13]. Thus, we have employed phosphonomethyl-amino acetic acid, $HO_2CCH_2NHCH_2PO_3H_2$ and imino-bis(methylphosphonic) acid, $H_2O_3PCH_2NHCH_2PO_3H_2$ in the synthesis of two new lead compounds, $Pb(O_3PCH_2NH_2CH_2COO)$ and $Pb(HO_3PCH_2NHCH_2PO_3H)$ [14].

As part of our ongoing investigation of metal phosphonates we describe here the use of a tetraphosphonic acid to expand further the phosphonate chemistry and report the synthesis and characterization of the first manganese tetraphosphonate, $Mn[(HO_3PCH_2)_2N(H)(CH_2)_4(H)N(CH_2PO_3)_2]$.

2. Experimental

2.1. Synthesis

The tetraphosphonic acid, $(H_2O_3PCH_2)_2N–(CH_2)_4–N(CH_2PO_3H_2)_2$, has been synthesized by a Mannich-type reaction starting from 1,4-diaminobutane, phosphonic acid and formaldehyde. In a 250 mL three-neck flask a mixture of 0.1 mol 4-aminobutylamine (8.8 g) and 0.4 mol solid phosphorous acid (32.8 g) were dissolved in mixture of 40 mL water and 40 mL hydrochloric acid. After heating the solution to reflux 60 mL of an aqueous 37% formaldehyde solution (0.8 mol) were added within 60 min. The solution was kept under reflux for additional 60 min and was then cooled to room temperature. Filtration of the crude product and recrystallization from dilute hydrochloric acid gave 38 g (82%) pure product as colorless crystals.

$Mn[(HO_3PCH_2)_2N(H)(CH_2)_4(H)N(CH_2PO_3H)_2]$ was synthesized at 150°C as a single phase product by hydrothermal reaction of 29.8 mg (0.064 mmol) $(H_2O_3PCH_2)_2N–(CH_2)_4–N(CH_2PO_3H_2)_2$ with 49.7 mg (0.25 mmol) $MnCl_2 \cdot 4H_2O$ (Aldrich) mixed in 5.3 g water. The pH of the solution was adjusted to pH 6 using 0.1 M NaOH. The reaction mixture was stirred to homogeneity, transferred to a 23 mL Teflon liner and sealed in a stainless-steel autoclave (Parr, USA). The reaction was carried out at 150°C for 11 days under autogeneous pressure. The resulting single phase product was filtered and washed thoroughly with deionized water and acetone. The pH of the final solution was pH = 1. The product was composed of a microcrystalline powder and some needle-like crystals. X-ray powder diffraction experiments confirmed the presence of only one phase, $Mn[(HO_3PCH_2)_2N(H)(CH_2)_4(H)N(CH_2PO_3H)_2]$. In order to investigate the influence of the molar ratio Mn:tetraphosphonic acid in the starting mixture, reactions were performed in an eight-hole reactor developed in our group [15]. The molar ratio was varied between 1:4 and 4:1 and the reactions were carried out at the same conditions as mentioned above. After work-up by centrifugation and characterization by automated X-ray powder diffraction, all eight products were identified as microcrystalline $Mn[(HO_3PCH_2)_2N(H)(CH_2)_4(H)N(CH_2PO_3H)_2]$. No additional phase was observed.

2.2. Physical characterization

Thermogravimetric analysis was performed on a thermal analyzer (Netzsch STA 409) under air (40 $cm^3\,min^{-1}$, heating rate: 10°C min^{-1}). As can be seen in Fig. 1 the sample is stable up to ~290°C and only a small weight loss between room temperature and 110°C is observed which is probably due to adsorbed water on the surface of the crystallites. Between 290°C and 345°C a one-step loss of ~7.0% is observed, which could correspond to the departure of two water molecules per formula unit (calcd. 6.5%), due to the presence of hydrogenphosphonate groups. Above 345°C the continuous decomposition of the organic part of the structures takes place. The magnetic susceptibility data for the title compound were recorded over the temperature range 2–300 K using a SQUID magnetometer, Quantum Design Model 1802. The microcrystalline sample was zero-field cooled (z.f.c.) to 2 K and the magnetization was measured on heating to 300 K in an applied field of 1000 G.

2.3. X-ray structure determination

The single-crystal structure determination by X-ray diffraction was performed on an Enraf-Nonius Kappa-CCD diffractometer equipped with a rotating anode (Mo$K\alpha$ radiation, $\lambda = 0.71073$ Å) operating at 55 kV and 75 mA. Powder X-ray diffraction patterns were recorded on a STOE STADI-P instrument equipped with an $x-y$ stage and an image plate detector using Cu$K\alpha$ radiation.

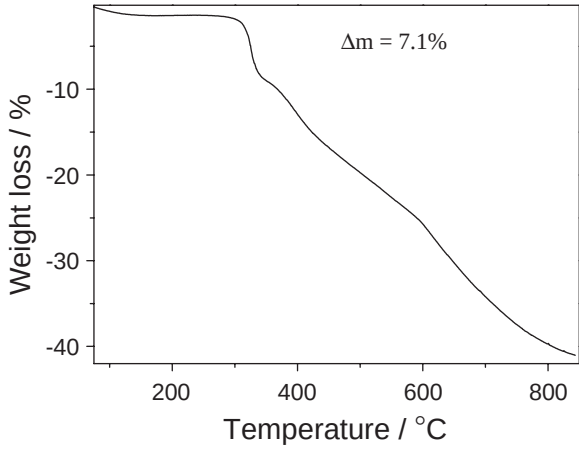

Fig. 1. TG measurement of the title compound (flow gas: air, heating rate: 10°C min^{-1}).

Table 1
Summary of the crystallographic data

Empirical formula	$Mn[(HO_3PCH_2)N(H)(CH_2)_4(H)N(CH_2PO_3H)_2]$
Space group	$P2_1/a$
a (Å)	9.6663(1)
b (Å)	9.2249(2)
c (Å)	10.5452(1)
β (deg)	105.676(1)
Volume (Å^3)	905.35(2)
Z	2
Formula mass	517.10
ρ (g cm^{-3})	1.897
Crystal size (μm^3)	$0.11 \times 0.1 \times 0.02$
μ (mm^{-1})	1.148
2θ range (deg)	8.0, 60.1
Range in $h\,k\,l$	$-13 \leqslant h \leqslant 13$, $-12 \leqslant k \leqslant 12$, $-14 \leqslant l \leqslant 14$
Total data collected	16732
Unique/obs. data ($I > 2\sigma(I)$)	2617/2210
Extinction coefficient	0.007(2)
R_{int}	0.0502
Absorption correction	Numerical
$T_{min.}/T_{max.}$	0.8135/0.9731
R_1, wR_2 ($I > 2\sigma(I)$)	0.040, 0.1021
R_1, wR_2 (all data)	0.051, 0.1083
Goodness of fit	1.061
No. of variables	140
Δe min/max (e Å^{-3})	−0.742/1.622

Table 2
Atomic coordinates and equivalent isotropic displacement parameters (Å^2) for $Mn((HO_3PCH_2)_2N(H)–C_4H_8–(H)N(CH_2PO_3H)_2)$. U_{eq} is defined as one-third of the trace of the orthogonalized U_{ij} tensor

Atom	x	y	z	U_{eq}
Mn1	0.0000	0.0000	0.0000	0.01389(14)
P1	0.22876(6)	0.28195(6)	0.04807(5)	0.01511(15)
P2	0.00836(7)	0.09088(7)	−0.31185(6)	0.02193(17)
O1	0.1963(2)	0.3561(2)	0.17081(18)	0.0266(4)
H1	0.263(4)	0.371(4)	0.216(3)	0.032
O2	0.19453(17)	0.12326(18)	0.04482(17)	0.0200(3)
O3	0.37675(17)	0.31717(17)	0.03778(16)	0.0186(3)
O4	−0.0986(2)	0.1552(2)	−0.43828(17)	0.0273(4)
H4	−0.080(2)	0.122(3)	−0.499(3)	0.033
O5	0.0789(2)	−0.0443(2)	−0.34471(18)	0.0305(4)
O6	−0.06716(18)	0.08072(18)	−0.20580(15)	0.0205(3)
N1	0.1369(2)	0.3671(2)	−0.21571(19)	0.0198(4)
H1n	0.2078	0.4069	−0.2072	0.024
C1	0.0972(2)	0.3713(3)	−0.0870(2)	0.0181(4)
H1B	0.0046	0.3247	−0.0988	0.022
H1A	0.0874	0.4716	−0.0632	0.022
C2	0.1601(3)	0.2159(3)	−0.2617(2)	0.0231(5)
H2B	0.2322	0.1696	−0.1912	0.028
H2A	0.2013	0.2258	−0.3355	0.028
C3	0.0283(3)	0.4540(3)	−0.3171(2)	0.0259(5)
H3B	0.0233	0.5510	−0.2832	0.031
H3A	−0.0655	0.4097	−0.3306	0.031
C4	0.0633(3)	0.4647(4)	−0.4498(3)	0.0346(6)
H4A	0.0807	0.3688	−0.4798	0.041
H4B	0.1493	0.5225	−0.4407	0.041

Table 3
Bond lengths (Å) and angles (°) for $Mn((HO_3PCH_2)_2N(H)–C_4H_8–(H)N(CH_2PO_3H)_2)$

Mn1–O2 (2 ×)	2.138 (2)	Mn1–O6 (2 ×)	2.219 (2)
Mn1–O3 (2 ×)	2.163 (2)	P1–C1	1.829 (2)
P1–O1	1.569(2)	P2–C2	1.828(3)
P1–O2	1.499(2)	C1–N1	1.508(3)
P1–O3	1.499(2)	C2–N1	1.513(3)
P2–O4	1.566(2)	N1–C3	1.510(3)
P2–O5	1.506(2)	C3–C4	1.529(4)
P2–O6	1.495(2)	C4–C4	1.530(5)
O–Mn1–O(12 ×)	83.6 (1)–96.4 (1)	P1–C1–N1	113.39 (15)
O–Mn1–O(3 ×)	180.0(1)	P2–C2–N1	119.83(16)
O1–P1–O2	110.6(2)	O4–P1–O5	110.7(2)
O1–P1–O3	111.9(2)	O4–P1–O6	108.5(2)
O2–P1–O3	114.8(2)	O5–P1–O6	117.6(2)
C1–P1–O1	101.2(2)	C2–P2–O4	107.5(2)
C1–P1–O2	108.6(2)	C2–P2–O5	102.2(2)
C1–P1–O3	108.8(2)	C2–P2–O6	109.8(2)
N1–C3–C4	113.6(2)	C–N1–C	113.4(2)–114.1(2)

A suitable single crystal was carefully selected under a polarizing microscope. For data reduction the programs HKL Denzo and Scalepack [16] were used and the absorption correction was carried out using Xred [17]. The single-crystal structures were solved by direct methods and refined using the programs SHELXS and SHELXL [18]. The refinement converged without any problems and all H-atoms were located from the difference Fourier maps. These H-atoms were refined using a riding model and fixing the temperature factor to be 1.2 times the value of the oxygen or nitrogen atom they are bonded to.

Experimental data and results of the structure determination are given in Table 1. Atomic coordinates with isotropic displacement parameters are shown in Table 2, and the bond angles and bond distances are summarized in Table 3. CCDC 206624 contains the supplementary crystallographic data for this paper. These data can be obtained free of charge via www.ccdc.cam.ac.uk/conts/retrieving.html (or from the CCDC, 12 Union Road, Cambridge CB2 1EZ, UK; fax: +44-1223-336033; mailto:deposit@ccdc.cam.ac.uk).

3. Results and discussion

3.1. Synthesis

The title compound $Mn[(HO_3PCH_2)_2N(H)(CH_2)_4(H)N(CH_2PO_3H)_2]$ has been obtained as single-phase microcrystalline as well as coarse crystalline product. Although the molar ratios $Mn:(H_2O_3PCH_2)_2N–(CH_2)_4–N(CH_2PO_3H_2)_2$ were varied from 1:4 to 4:1 the title compound was always obtained as the only crystalline product.

3.2. X-ray crystal structure

The asymmetric unit is shown in Fig. 2. The three-dimensional structure is composed of Mn^{2+} ions and zwitter ions $[(HO_3PCH_2)_2N(H)(CH_2)_4(H)N(CH_2PO_3H)_2]^{2-}$ where each phosphonate group and each N-atom is protonated by one H-Atom. The positions of the hydrogen atoms were unambiguously derived from the single-crystal structure determination. The coordination behavior of the tetraphosphonic acid and the Mn(II) ion is shown in Figs. 3 and 4, respectively. The oxygen atoms of tetraphosphonic acid unit act as chelating as well as a monodentate ligand (Fig. 3). All oxygen atoms that are involved in the coordination are only binding to a single Mn^{2+} ion (μ_2 oxygen). Each Mn^{2+} ion is surrounded by six phosphonate oxygen atoms of six different hydrogen phosphonate groups thus forming the typical MnO_6 octahedra. In contrast to many M^{2+} phosphonates (M = Mg, Mn, Zn, Ca, Cd) [19], where two oxygen atoms of the phosphonate groups chelate to the metal while at the same time the chelating oxygens bridge to adjacent metal atoms, we find that here the Mn^{2+} ion

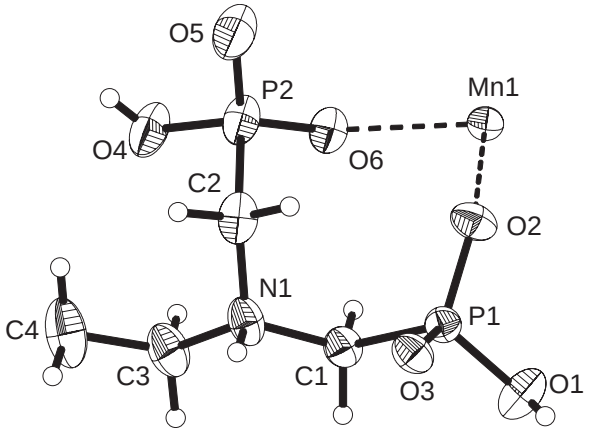

Fig. 2. Asymmetric unit of $Mn[(HO_3PCH_2)_2N(H)–C_4H_8–(H)N(CH_2PO_3H)_2]$. Thermal ellipsoids are shown at the 75% probability level.

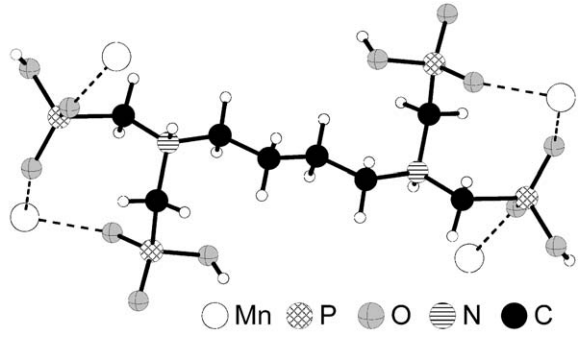

Fig. 3. Coordination behavior of zwitter-ion $[(HO_3PCH_2)_2N(H)–C_4H_8–(H)N(CH_2PO_3H)_2]^{2-}$.

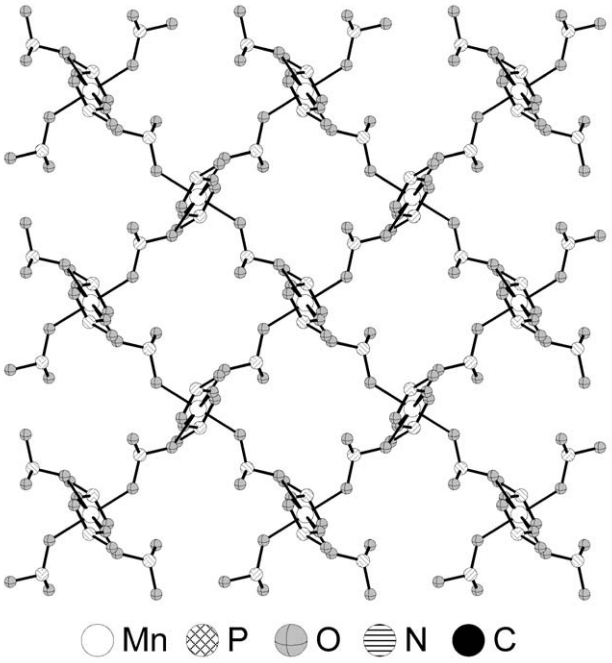

Fig. 4. Connection of the MnO_6 and PO_3C polyhedra forming nets of eight-rings in the a,b-plane.

are surrounded by six phosphonate groups in the second coordination sphere (Fig. 4). The almost ideal MnO_6 polyhedra (d(Mn–O) = 2.138(2)–2.219(2) Å; O–Mn–O angles: 180.0(1) (3 ×), 83.6(1)–96.4(1) (12 ×)) are in full agreement with the sum of the ionic radii Mn^{2+} and O^{2-} (97 + 122 = 219 pm) [20] and values observed in other Mn phosphates and phosphonates ($(Mn_2(PO_4)(OH)$: d(Mn–O) = 210.9–223.5 pm; β'-$Mn_3(PO_4)_2$: d(Mn–O) = 212.6–224.2 pm; $Mn_3(O_3PCH_2CH_2COO)_2$: d(Mn–O) = 203.2(8)–225.3(7) pm). The MnO_6 polyhedra are connected by the phosphonate groups forming layers in the a,b-plane (Fig. 4). Thus eight-rings are formed by alternating MnO_6 and PO_3C polyhedra. The layers are connected by the organic groups, $(–CH_2)_2N(H)–(CH_2)_4–(H)N(CH_2–)_2$ thus blocking the eight-rings apertures (Figs. 5 and 6). The structure is further stabilized by extensive N–H ···O and O–H···O hydrogen bonding (Fig. 5). Thus all OH groups and the NH group take part in the hydrogen bonding scheme. The H-atoms of the hydrogen phosphonate groups are attached to the O-atoms O1 and O4. The O-atoms O2, O3 and O6 are the only ones coordinated to the Mn^{2+} ion as μ_2-atoms, and O5 acts twice as the H acceptor (O1···O5: 2.603 Å, O4···O5: 2.561 Å). The H atom H1 is also involved in the hydrogen bonding scheme and a N1–H1···O6 bond is observed (N1···O6: 2.875 Å). The H-bonding scheme is also reflected in the P–O distances. Whereas for the P–OH distances values of 1.566(2) and 1.569(2) Å are observed, shorter bonds (1.495(2)–1.506(2) Å) are found for the other P–O

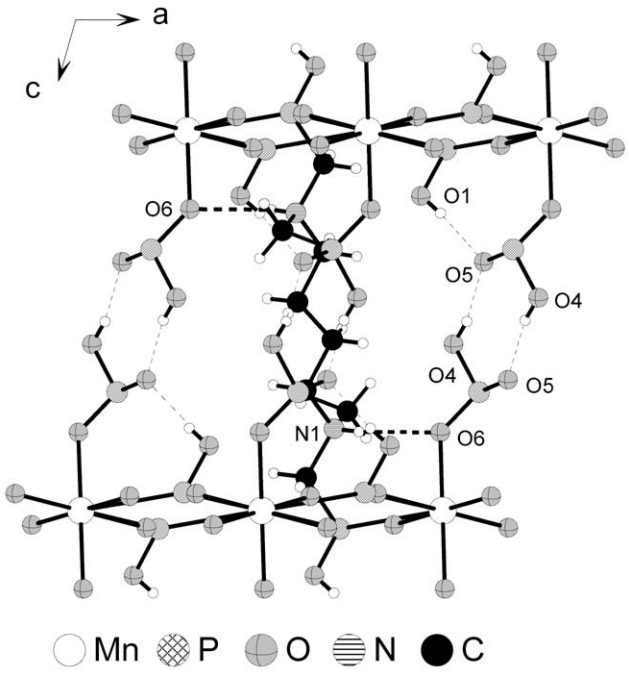

Fig. 5. Connection of the Mn,P,O-layers by the tetramethylendiaminobutane groups and O–H···O hydrogen bonds (thin dotted lines). N–H···O hydrogen bonds are presented by bold dotted lines.

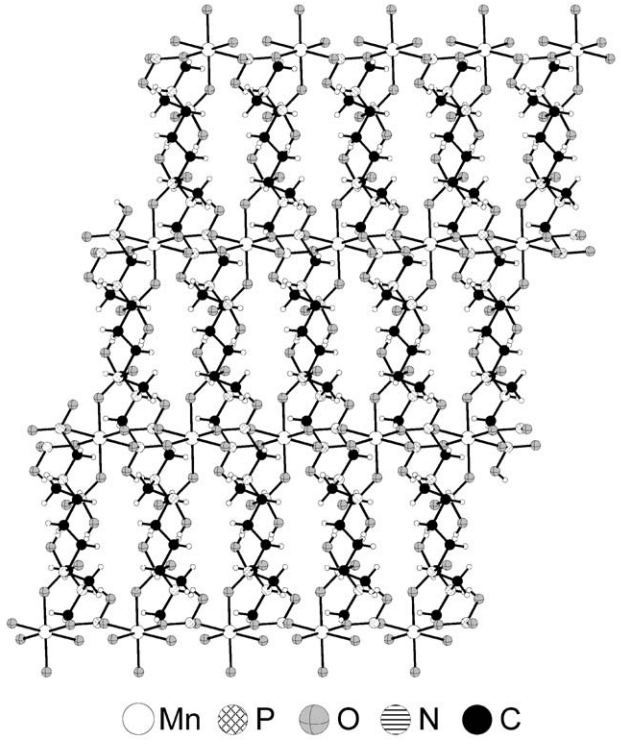

Fig. 6. Structure of $Mn[(HO_3PCH_2)_2N(H)–C_4H_8–(H)N(CH_2PO_3H)_2]$. View along [010].

distances. These values are in agreement with literature data where for P═O bonds values of 1.51(1) are expected [21].

3.3. Magnetic properties

The magnetic studies were undertaken in order to confirm the +2 oxidation state of Mn and to determine if $Mn[(HO_3PCH_2)_2N(H)(CH_2)_4(H)N(CH_2PO_3H)_2]$ exhibits any interesting magnetic properties. The title compound displays a Curie–Weiss behavior over a wide range of temperatures having a Weiss constant of $\theta = -15.9\,K$. The effective magnetic moment of $5.97\,\mu_B$ is consistent with high-spin Mn^{2+} ions (d^5) in octahedral environments (expected: $5.92\,\mu_B$).

Acknowledgments

The authors thank Dr. R.-D. Hoffmann and Prof. Dr. R. Pöttgen for the magnetic measurements and the BMBF for partial funding of the work (03C0309D). N. Stock wishes to thank the "Fond der Chemischen Industrie" for financial support.

References

[1] A.K. Cheetham, G. Férey, T. Loiseau, Angew. Chem. Int. Ed. 38 (1999) 3268.
[2] (a) A. Clearfield, Chem. Mater. 10 (1998) 2801.
(b) M.B. Dines, P.M. DiGiacomo, Inorg. Chem. 20 (1981) 92.
[3] (a) A. Distler, L. Lohse, S.C. Sevov, J. Chem. Soc. Dalton Trans. (1999) 1805.
(b) V. Soghomonian, Q. Chen, R.C. Haushalter, J. Zubieta, Angew. Chem. Int. Ed. 34 (1995) 223.
(c) C. Serre, G. Férey, Inorg. Chem. 38 (1999) 5370.
(d) R. LaDuca, D. Rose, J.R.D. DeBord, R.C. Haushalter, C.J. O'Connor, J. Zubieta, J. Solid State Chem. 123 (1996) 408; D.L. Lohse, S.C. Sevov, Angew. Chem. Int. Ed. 36 (1997) 1619.
[4] S. Drumel, P. Janvier, D. Deniaud, B. Bujoli, J. Chem. Soc. Chem. Commun. (1995) 1051.
[5] (a) N. Stock, S. Frey, G.D. Stucky, A.K. Cheetham, J. Chem. Soc. Dalton Trans. (2000) 4292.
(b) N. Stock, G.D. Stucky, A.K. Cheetham, J. Chem. Soc. Chem. Commun. (2000) 2277.
[6] A. Cabeza, M.A.G. Aranda, S. Bruque, J. Mater. Chem. 9 (1999) 571.
[7] C.V.K. Sharma, A. Clearfield, J. Am. Chem. Soc. 123 (2001) 2885.
[8] A. Cabeza, S. Bruque, A. Guagliardi, M.A.G. Aranda, J. Solid State Chem. 160 (2001) 278.
[9] H.S. Martinez-Tapia, A. Cabeza, S. Bruque, P. Pertierra, S. Garcia-Granda, M.A.G. Aranda, J. Solid State Chem. 151 (2000) 122.
[10] E. Irran, N. Stock, T. Bein, J. Solid State Chem., in press.
[11] N. Stock, N. Guillou, T. Bein, G. Férey, Solid State Sci. 5 (2003) 629.
[12] N. Stock, T. Bein, J. Solid State Chem. 167 (2002) 330.
[13] K. Moedritzer, R.R. Irani, J. Org. Chem. 31 (1966) 1603.
[14] N. Stock, Solid State Sci. 4 (2002) 1089.
[15] K. Choi, D. Gardner, N. Hilbrandt, T. Bein, Angew. Chem. Int. Ed. 38 (1999) 2891.

[16] Z. Otwinowski, W. Minor, Methods in enzymology, in: C.W. Carter, R.M. Sweet (Eds.), Macromolecular Crystallography, Part A, Vol. 276, Academic Press, New York, 1997, pp. 307–326.
[17] XRED, Data reduction and absorption correction program version 1.09 for Windows, Stoe & Cie GmbH, Darmstadt, 1997.
[18] G.M. Sheldrick, SHELXS-97, Program for the solution of crystal structures, Universität Göttingen 1997;
G.M. Sheldrick, SHELXL-97, Program for the refinement of crystal structures, Universität Göttingen, 1997.
[19] G. Cao, H. Lee, V.M. Lynch, T.E. Mallouk, Inorg. Chem. 27 (1988) 2781.
[20] R.D. Shannon, Acta Crystallogr. A 32 (1976) 751.
[21] D.E.C. Corbridge, Phosphorus, Elsevier, Amsterdam, 1990, p. 47.